ORIGINAL PAPER

The potential growth and lipid accumulation in *Coccomyxa subellipsoidea* triggered by glucose combining with sodium acetate

Zhenyao Wang[1] · Fei Luo[1] · Ziting Wang[1] · Rong Zhou[1] · Yufang Tang[1] · Yuqin Li[1]

Abstract

Carbon sources whether types or magnitudes were fateful in terms of stimulating growth and lipids accumulation in microalgae applied for biodiesel production. The set scenario of this work was to investigate the feasibilities of glucose (G) combining with sodium acetate (SA) carbon sources in enhancing biomass and lipid accumulation in *Coccomyxa subellipsoidea*. The results demonstrated that *C. subellipsoidea* subjected to the combination feeding of G (20 g/L) and SA (12 g/L) achieved the favorable biomass (5.22 g/L) and lipid content (52.16%). The resulting lipid productivity (388.96 mg/L/day) was 1.33- to 7.60-fold more than those of sole G or SA as well as other combinations of G and SA. Even though the total fatty acids of *C. subellipsoidea* cells treated with the optimal combination of G and SA showed no noticeable increment in comparison with sole G or SA, the proportion of monounsaturated C18:1 (over 48.69%) and the content of C18:3 (< 12%) were commendable in high-quality algal biodiesel production. Further, such fascinating lipid accumulation in *C. subellipsoidea* cells treated with G combining with SA might be attributed to that G promoted glycolysis as well as SA activated glyoxylate shunt and TCA cycle to synergistically provide sufficient acetyl-CoA precursors for lipid accumulation. These findings hinted the potential of the combination of carbon sources in enhancing the overall lipid productivity to offset alga-based biodiesel production cost and would guide other alga strains cultivation.

Keywords Biomass · *Coccomyxa subellipsoidea* · Glucose · Lipid productivity · Metabolites · Sodium acetate

Introduction

The unceasing emission of greenhouse gases and depletion of fossil fuels promoted exploitation of renewable and environmentally-friendly bioenergy sources. Biodiesel as a carbon-neutral and sustainable alternative to fossil fuels attracted increasing attention. However, biodiesel derived from traditional oil crops (e.g. rapeseed, soybean, and sunflower seed) could not satisfy even a small fraction of the existing demand for transport fuels. Microalgae endowed with rapid growth rate, higher energy-conversion efficiency, areal oil yields, and no competition with food crops and agricultural land were praised as a promising feedstock for biodiesel production (Demirbas 2010; Shuba and Kifle 2018).

The benefits of microalgae notwithstanding, algae-based biodiesel was still uncompetitive with petroleum fuels due to the low lipid productivity and the high lipid production cost per unit volume.

Enhancing the lipid productivity of microalgae might be the most workable and fundamental strategy to down-regulate the cost of alga-based biodiesel. Heterotrophic regime was always taken delight in eliminating light requirements as well as requiring only organic compounds as carbon and energy sources to produce microalgal lipids. While carbon sources whether types or magnitudes employed in heterotrophic cultivation process was crucial in terms of stimulating growth and lipids formation in microalgae (Perez-Garcia et al. 2011). Reflecting upon the majority of publications, glucose as carbon and energy source was frequently used by microalgae during heterotrophic process (Silva et al. 2016). However, glucose fermentation carbon substrate accounting for approximate 80% of total cost consequently limited the industrialization of heterotrophic microalgae (Yu et al. 2018). In order to further popularize heterotrophic regime, many endeavors were concentrating on finding some

✉ Rong Zhou
zhourong2018@xtu.edu.cn

✉ Yuqin Li
yuqinli2004@126.com

[1] School of Chemical Engineering, Xiangtan University, Xiangtan 411105, People's Republic of China

inexpensive materials including carbon-rich wastes or low-grade biomass instead of glucose for cultivating microalgae (Wen et al. 2013; Mu et al. 2015; Wang et al. 2018). Acetate as the most common two-carbon building blocks for biosynthesis in organisms was especially popular since it could ensure the cost-competitive lipid production. And also applying acetate as carbon source for culture of microalgae would be advantageous to maintain axenic heterotrophic cultures since many bacteria could not utilize acetate as carbon source. However, some biochemical indicators including the growth rate, the dry biomass, and adenosine triphosphate (ATP) generated by acetate might be significantly lower than glucose cultures. Actually, each carbon feedstock implemented different metabolic behaviors to cause lipid accumulation in microalgae at different degree, an unambiguous conclusion about which carbon feedstock would be used to industrialization were still be non-uniform.

Combining multiple carbon sources for microalgae cultivation was advocated not only in reducing lipid production cost but also further improve microalgal lipid productivity. However, the combination formulation of carbon sources in the medium must satisfy the basic requirements for cell build-up and metabolite production by providing an adequate supply of energy for biosynthesis and cell maintenance. Another essential principle for the combination of carbon sources was that such a combination could exert the advantages of each carbon source or mutual complementation between carbon sources. Since the excellent characteristics of glucose or acetate as carbon source for heterotrophic cultivation of microalgae (Palabhanvi et al. 2016; Yang et al. 2018), some studies proposed that the combination of such two carbon sources might be an ideal solution in obtaining the high cell production. Azma et al. (2011) found that the cell yield of heterotrophic *Tetraselmis suecica* by glucose combining with acetate in medium was approximate 3.0-fold in comparison with non-combined carbon sources; Marudhupandi et al. (2016) reported that applying glucose combining with acetate as carbon source yielded the high biomass and lipid content in heterotrophic *Nannochloropsis salina*; another representative example was that a combination of acetic acid and glucose as carbon source not only maintained the almost constant pH value but also significantly increased the total biomass production of *Chlorella* (Huang et al. 2017). Although glucose combining with acetate had better performance in cell production of aforementioned microalgae strains, the specific coupling mechanisms in stimulating intracellular substances formation as well as whether or not applicable in any given microalgae were still unclear.

Alga species selection as the starting point of algal production pipeline was fundamentally important since this would determine the economic viability of the biodiesel process to some extent (Oh et al. 2018). Currently, many algal species such as *Xantophyta*, *Chrysophyta*, *Bacillariophyta*, *Phaeophyta*, *Rhodophyta*, and *Chlorophyta* have been examined with lipid yield and subsequently used for biodiesel production (Nascimento et al. 2013). However, amongst these tested microalgae, a considerable algal biomasses were easy to culture but contained a low oil content or achieved the high lipid content with the high cultivation cost, which rendered the microalgae conversion to biofuels little profitable and rewarding. The polar microalgal *Coccomyxa subellipsoidea* was regarded as a new candidate for biodiesel production due to fragile cell wall to easily releasing contents, the high growth rate as well as known fully sequenced genome (Peng et al. 2016). Moreover, *C. subellipsoidea* from the polar environment was more helpful to reduce cultivation cost because controlling cultivation temperature to maximize the growth rate would be a major energy expense in large-scale production (Allen et al. 2017). Therefore, some related works including evaluating the potential of biodiesel derived from *C. subellipsoidea* and cultivation strategies were sequentially implemented (Allen et al. 2015; Yu et al. 2018). However, the formulation of glucose combining with acetate for improvement of heterotrophic cultivation of *C. subellipsoidea* was rarely reported in the literatures. The objective of this study was to investigate the feasibilities of glucose combining with sodium acetate on the biomass and lipid production in *C. subellipsoidea*. The biomass, lipid productivity, and fatty acid profiles would be employed to verify the optimal combination of glucose and sodium acetate and identify biochemical properties that resulted in accumulation of lipids in heterotrophic *C. subellipsoidea*. The resulting results were expected to guide other algal strains cultivation and also offset algal-based biodiesel production cost.

Materials and methods

Materials

The microalgal strain *Coccomyxa subellipsoidea* C-169 was a gift from South China University of Technology (SCUT), China. The tested *Coccomyxa subellipsoidea* C-169 was a type of small elongated non-motile unicellular green alga and was from algal peat in polar Antarctica. Fatty acids standards (MIX C4-C24 Supelco Analytical) were purchased from Sigma Chemical Co (St. Louis, MO, USA). All other chemicals were of the highest purity available.

Microalgae cultivation

For routine sterile operations, a single colony from the stock agar plate was picked and inoculated into 30 mL of liquid Basal medium containing the following ingredients (per L): 1 g $MgSO_4 \cdot 7H_2O$, 1.25 g KH_2PO_4, 0.5 g EDTA, 114.2 mg

boron, 83.75 mg $CaCl_2$, 49.8 mg $FeSO_4 \cdot 7H_2O$, 38.2 mg $ZnSO_4 \cdot 7H_2O$, 15.7 mg $CuSO_4 \cdot 5H_2O$, 14.4 mg $MnCl_2 \cdot 4H_2O$, 7.1 mg MoO_3, 4.9 mg $CoNO_3 \cdot 6H_2O$, 1.5 g $NaNO_3$, and 10.0 g glucose. The liquid seed was cultured at 28 °C and constant light intensity of 50 μmol/m²/s to achieve approximate 5×10^5 cells/mL. Subsequently, 1 mL of the pre-cultured *Coccomyxa subellipsoidea* seed liquid was inoculated into 250 mL flask with 100 mL Basal medium and cultured with constant light intensity of 50 μmol/m²/s at 28 °C to obtain cell density of 8×10^5 cells/mL secondary algal seed. Subsequently, *C. subellipsoidea* cultivation experiments were performed under heterotrophic condition with glucose (G) combining with sodium acetate (SA) as carbon sources. The concentrations of G and SA were respectively set as 10, 20, 30 g/L and 6, 12, 18 g/L. As set in Table 1, totally nine trials would be carried out and each trial was three biological duplicates. Concretely, up to 10 mL of secondary algal seed was individually inoculated into 100 mL Basal medium supplemented with above nine different combinations of G and SA carbon sources instead of initial 10.0 g/L of glucose. All inoculated cultures were heterotrophically cultured on a reciprocating shaker (160 rpm/min) at 28 ± 1 °C without light exposure for 168 h. Finally, the algal liquid were centrifuged and collected to determine the biomass and lipid content biological indicators. Cultures with sole G (20 g/L) and sole SA (12 g/L) carbon source were respectively regarded as control groups.

Analysis methods

Biomass determination

All algal cultures (100 mL per sample) were collected at 168 h by centrifugation at 6000 rpm for 30 min and washed several times with distilled water. The wet algal pellets were then lyophilized until constant weight and the biomass was determined by the cell dry weight method. The specific growth rate of algal cultures was obtained by the following calculation:

$$\mu(d^{-1}) = \frac{\ln N_t - \ln N_0}{t}$$

where N_0 and N_t indicated the biomass concentration (g/L); t represented biomass concentration determination time interval (d).

Total lipid content

Up to 20 mg of the lyophilized algal powder was blended with 0.5 mL distilled water and disrupted using a microwave oven at 100 °C and 2450 MHz for 5 min. Totally 3 mL of chloroform/methanol (2:1, V/V) was then introduced into the mixtures and tempestuously shaken by hybrid oscillator for 20 min. The chloroform/methanol extraction procedure was performed three to five times. All the chloroform phases were collected by centrifugation at 6000 rpm/min for 30 min and evaporated by nitrogen blowing concentrators. The lipid content was measured by the lipid weight divided by cell dry weight and was expressed as %.

Fatty acids composition and content

The fatty acids profiles in lipid were analyzed by gas chromatography linked mass spectrometry (GC–MS). The freeze-dried algal powdered sample was firstly saponified by NaOH–CH₃OH solution at 85 °C in a thermostated water bath for 1 h. Totally 2 mL of boron trifluoride/methanol (1:2, V/V) was then introduced into saponified solutions and vortexed for 30 min. Subsequently, the saponified solutions were dissolved in 2 mL of hexane to extract the resulting fatty acid methyl esters (FAMEs). Up to 10 μL of 100 μg/mL 2-chloronaphthalene was added to 90 μL of FAMEs before GC–MS analysis. Samples were analyzed by using a gas chromatograph (model 7890A, Agilent Technologies) equipped with a mass-selective detector (model 5975C, Agilent Technologies), an autosampler (7683B series, Agilent Technologies), a split/splitless injector, an injection module, and ChemStation software. A capillary column (Agilent DB-23; 30 m × 0.25 mm × 0.25 μm) and helium as the carrier gas at a flow rate of 1.00 mL/min were used. Samples were injected in split mode (5:1 split ratio) with an injection volume of 1.0 μL. The oven temperature program consisted of an initial hold at 45 °C for 2.0 min, ramping to 150 °C within 15 min then to 240 °C within 30 min, and a final hold at 240 °C for 3 min. FAMEs were identified by autoscan and direct comparison of their mass spectral pattern, and the retention index was determined with the NIST08.LIB mass spectral database. FAMEs were quantified by using a FAME mixture standard with C17:0 as the internal standard.

Table 1 Different combination of glucose and sodium acetate for heterotrophic cultivation of *C. subellipsoidea*

Trials	Glucose (G) (g/L)	Sodium acetate (SA) (g/L)	Combination mode
1	10	6	10 G + 6 SA
2	10	12	10 G + 12 SA
3	10	18	10 G + 18 SA
4	20	6	20 G + 6 SA
5	20	12	20 G + 12 SA
6	20	18	20 G + 18 SA
7	30	6	30 G + 6 SA
8	30	12	30 G + 12 SA
9	30	18	30 G + 18 SA

Ultrastructure analysis

The algal cells were collected by centrifugation at 6000 rpm at 4 °C for 30 min and then fixed in a solution of 3% glutaraldehyde in distilled water for 2 h at 4 °C. The glutaraldehyde-fixed cells were centrifuged at 4 °C and suspended in 0.1 M phosphate buffer accompanied with periodic agitation at 10 min intervals. The cells were post-fixed for 90 min at 4 °C in 1% osmium tetraoxide. The cell samples were dehydrated by incubation in a graded series of 30%, 50%, 70%, 80%, 90%, and 100% ethanol. Subsequently, the embedding solution composed of propylene oxide and epoxy resin (2:1, v/v) was introduced into the dehydrated algal cells and incubated for 20 min. such process was repeated twice. Propylene oxide was removed via 4 h of vacuum pumping. The embedded cell samples were dried in oven at 70 °C until the epoxy was thoroughly polymerized. The dried algal cell samples were performed ultrathin sectioning as well as staining by uranyl acetate and lead citrate. The samples were finally dried at 60 °C and visualized using a JEM-1230 transmission electron microscope (JEOL).

Metabolomics analysis

The samples (control and experimental groups) used for metabolomics analysis were the same cells samples used for biomass and lipid content analysis. The algal cells were harvested by centrifugation at 6000 rpm for 30 min and then performed freeze drying. Up to 30 mg of flash frozen and lyophilized algae material was mixed with 20 μL of chlorphenylalanine (0.3 mg/mL) and cold mixture of methanol:water (V/V, 4:1) was added to achieve 1 mL total volume. Subsequently, 200 μL of chloroform was added to the mixtures and were incubated in a sonic ice water bath for 6 min (6 s on and 4 s off, 500 W). The supernatants were collected by centrifugation (13,000 rpm) for 15 min at 4 °C and filtered by a 0.45-μm pore-size PTFE membrane. The filtered metabolites were transferred into the liquid chromatograph vials and analyzed by ultra performance liquid chromatography (UPLC, Waters, Milford, MA, USA) coupled with a photo diodearray (PDA, Waters) detector and an orthogonal time-of-flight mass spectrometer (TOF–MS, LCT premier, Waters). ACQUITY UPLC BEH C8 (100 mm × 2.1 mm, 1.7 μm) and ACQUITY UPLC HSS T3 (100 mm × 2.1 mm, 1.8 μm) chromatographic column (Waters Corp., USA) were used for gradient elution of positive and negative ionization modes. The mobile phases of positive and negative ion were solvent A [water/formic acid (100:0.1 (v/v)] and solvent B [acetonitrile/formic acid (100:0.1 (v/v)] as well as solvent A1 (6.5 mM ammonium bicarbonate in Milli-Q water) and solvent B1 [6.5 mM ammonium bicarbonate and methanol/Milli-Q water (95:5 (v/v)]. Flow rate and injection volume of the positive and negative ion mode were 0.35 mL/min and 5 μL, respectively. The following gradient elution was applied for positive ion mode: 0–1 min 95% solvent A and 5% solvent B, 1–28 min decreased from 95 to 0% solvent A and from 5% up to 100% solvent B, 28–30 min from 0% up to 95% solvent A and decreased from 100 to 5%. The gradient elution of negative ion mode: 0–1 min 95% solvent A1 and 5% solvent B1, 1–28 min decreased from 95 to 0% solvent A1 and from 5% up to 100% solvent B1, 28–30 min from 0% up to 95% solvent A1 and decreased from 100 to 5% solvent B1. Raw data were firstly transformed into mzML format by MSconventer and then used to extract peaks with XCMS soft (Version 1.50.1). The qualitative analysis of metabolites was performed by comparing retention times and mass fragmentation patterns with a commercially available standard library, National Institute of Standards and Technology mass spectral library (NIST, 2005, Gaithersburg, MD). The quantitative analysis of metabolites was performed by normalizing each peak with the internal standards (IS). Multivariate statistical analysis was subsequently implemented. The data were set up to a kind of 2D matrix and then imported into the SIMCA Demo software package (Version 14.0, Umetrics AB, Sweden). Principal components analysis (PCA) was used to give an overall distribution of metabolites between samples as well as an partial least squares discriminant analysis (PLS-DA) was set up to distinguish the overall difference in the metabolic profiles between groups and find the differential metabolites between groups. The potentially biochemically significant metabolites were screened by VIP value > 1 of the first principal component of PLS-DA model and p value < 0.05 of t test. The differential metabolites was identified by searching https://www.hmdb.ca/ (The Human Metabolome Database) and https://metlin.scripps.edu/ (METLIN). Finally, the identified differential metabolites were imported into KEGG database (https://www.genome.jp/KEGG/pathway.html) to perform pathway enrichment analysis and further understand metabolic pathway changes in different samples.

Statistical analysis

Values are the mean ± SD from at least three independent experiments. Statistical comparisons of differences between groups were analyzed using the two-way analysis of variance (ANOVA) followed by Tukey's post hoc test for multiple comparisons. Statistical analysis were performed using the software package SPSS 16.0 and a P value of < 0.05 was considered significant.

Results

Influences of different combinations of glucose and sodium acetate on *C. subellipsoidea* biomass and lipid content

As depicted in Fig. 1a, the achieved biomass (4.15 g/L) of *C. subellipsoidea* cells treated with sole glucose (G) (20 g/L) was higher than the value by 1.35 g/L in sole sodium acetate (SA) (12 g/L) treatment cells, implying that G was an excellent carbon source than SA in promoting the growth of algal cells. More interestingly, the biomasses of *C. subellipsoidea* cells feed with all 9 combinations of G and SA showed significant increments than that of sole SA treatment cells (Fig. 1a). While in comparison with the biomass of algal cells treated with sole G, the biomasses of the combinations (10G + 6SA, 10G + 12SA, and 10G + 18SA) treatment were less than that of sole G, the biomass of 20G + 6SA treatment was approximately

equal to sole G feeding cells while the other combinations (20G + 12SA, 20G + 18SA, 30G + 6SA, 30G + 12SA, and 30G + 18SA) induced significant increments in biomasses. Especially, the biomass of algal cells treated with 20G + 12SA reached 5.22 g/L, representing 1.03- to 3.86-fold higher than other combinations of G and SA as well as sole G and sole SA. Additionally, the specific growth rate (0.97 day^{-1}) of 20G + 12SA-treated cells was also superior than other carbon source combinations (ranging from 0.78 to 0.85 day^{-1}) and were significantly higher than sole G or SA ($p < 0.05$) (Fig. 1b). Overall, the combined G and SA carbon source particularly the combinations of G ≥ 20 g/L and SA ≥ 12 g/L performed better than sole G or SA in stimulating the growth of algal cells.

It could be seen from Fig. 1c that the lipid contents in heterotrophic *C. subellipsoidea* cells showed no notable differences amongst 10G + 6SA, 30G + 18SA, and sole G carbon sources. Whereas the lipid contents of other combinations (10G + 12SA, 10G + 18SA, 20G + 6SA, 20G + 12SA, 20G + 18SA, 30G + 6SA, 30G + 12SA) showed significant
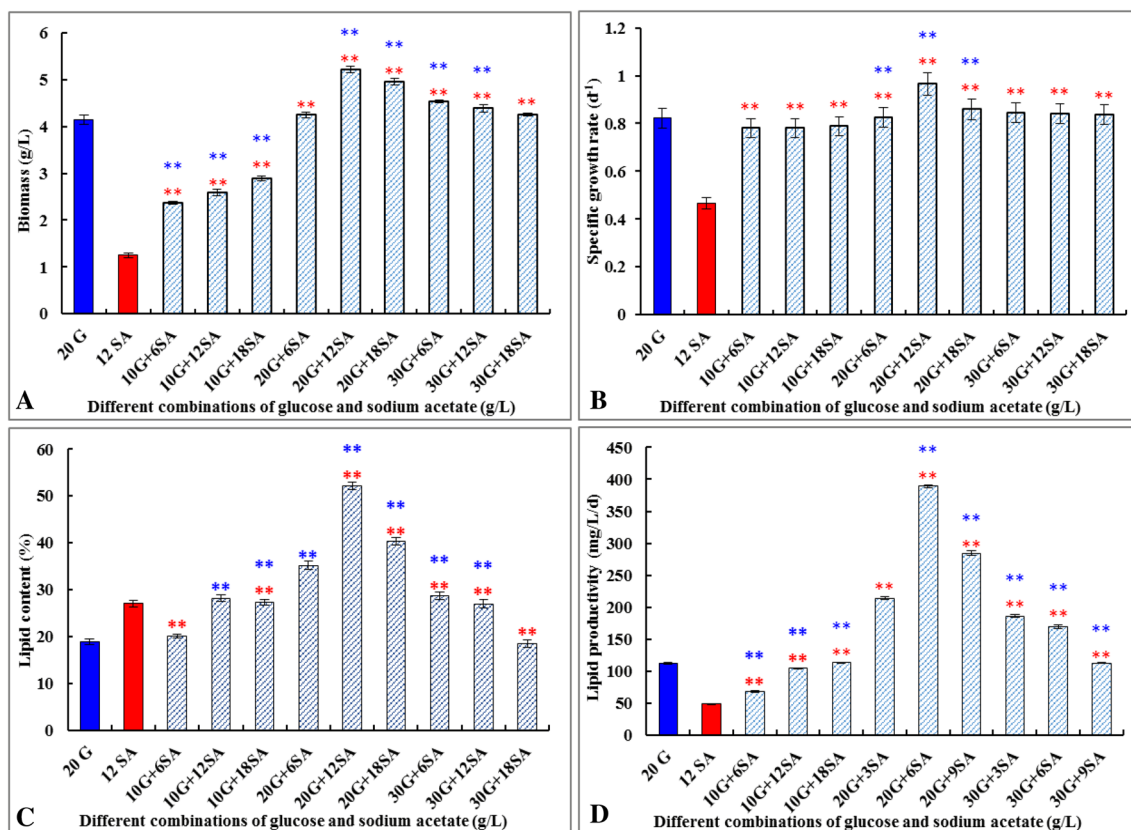

Fig. 1 Influences of different combinations of glucose and sodium acetate on biomass (**a**), specific growth rate (**b**), lipid content (**c**), and lipid productivity (**d**) of heterotrophic *C. subellipsoidea*. Glucose (G) and sodium acetate (SA) concentrations were specified in 10, 20, 30 g/L and 6, 12, 18 g/L, respectively. The numbers on the X-axis corresponded to the combinations and concentrations of G and SA

(e.g. 10G + 6SA indicated the combination of 10 g/L of G and 6 g/L of SA). Experiments were conducted with three biological replicates per treatment and the values represented the mean ± SD. **$p < 0.05$ compared with sole G (20 g/L) feeding cells (blue asterisk and blue column) or sole SA (12 g/L) feeding cells (red asterisk and red column)

increases than that of sole G carbon source. And the combination of 20G+12SA carbon source induced the highest lipid content (52.16%), which was 1.04- to 2.23-fold more than those of other combinations of G and SA and sole G. Although the biomass by sole SA treatment was lower than that of sole G, the lipid content responded to SA feeding showed 40.40% increase in comparison with sole G treatment. This indicated that SA carbon source might be more favorable lipid inducer than G carbon source. Moreover, the lipid contents of algal cells feed with 10G+12SA and 10G+18SA showed no substantial variations in comparison with sole SA carbon source. Even the lipid contents in *C. subellipsoidea* cells treated with 10G+6SA and 30G+18SA respectively showed 25.53% and 29.26% reduction than that of sole SA carbon source. However, the more optimistic cases were that the lipid contents ranged from 29.03% to 52.16% of *C. subellipsoidea* cells subjected to 20G+6SA, 20G+12SA, 20G+18SA, 30G+6SA, and 30G+12SA were significantly higher than that of SA treatment cells. Especially, the lipid content in 20G+12SA treatment cells was approximate 2.0-fold more than that of SA feeding cells. Collectively, the combination of G+SA carbon source particularly G≥20 g/L and 6 g/L≤SA≤12 g/L were more beneficial in stimulating lipid accumulation in heterotrophic *C. subellipsoidea*.

Even though the significant accumulation of lipid was implemented in sole SA treatment cells, this carbon source condition achieved 1.35 g/L of biomass and only resulted in 358.40 mg/L lipid yield and 51.2 mg/L/day lipid productivity, which was 1.67-fold and 2.19-fold less than that of sole G carbon source. And the lipid productivities by all of the combinations of G+SA were significantly higher than that of sole SA carbon source (Fig. 1d). Except for 10G+12SA, 10G+18SA, and 30G+18SA showing no significant variations as well as 10G+6SA showing significant reduction, the other combinations of 20G+6SA, 20G+12SA, 20G+18SA, 30G+6SA, and 30G+12SA achieved the more higher lipid productivities than that of sole G cells. While the combination of 20G+12SA carbon source induction not only simultaneously enhanced the biomass and lipid content but also ensured the highest lipid yield (2722.72 mg/L) and lipid productivity (388.96 mg/L/day), representing 1.33- to 7.60-fold more than those of other G+SA combinations as well as sole G and SA carbon sources. Therefore, given both of the biomass and lipid content biological indicators, the combination of 20G+12SA might be preferable option in terms of improving lipid productivity of heterotrophic *C. subellipsoidea*.

Influences of different combinations of glucose and sodium acetate on fatty acid profiles of *C. subellipsoidea*

Although the better performance of the combination of 20 g/L of glucose (G) and 12 g/L of sodium acetate (SA)

(G+SA) on the lipid productivity of heterotrophic *C. subellipsoidea*, it was still needed to detect the fatty acids whether or not comply with the established quality specifications of biodiesel. The fatty acid profiles of *C. subellipsoidea* cells treated with sole G, sole SA, and the combination of G+SA (respectively noted as G-cells, SA-cells, and G+SA-cells) were summarized in Table 2. Interestingly, no substantial differences in fatty acid profiles including length of carbon chain and degree of saturation were observed in G-cells, SA-cells, and G+SA-cells, being mainly composed of C16-C18 fatty acids ranging from 84.01% to 89.88% (Table 2). While the proportions of individual fatty acids were significantly different amongst G-cells, SA-cells, and G+SA-cells. Concretely, the palmitoleic acid (C16:1), hexadecadienoic acid (C16:2), and hexadecatrienoic acid (C16:3) in G-cells accounted for 4.40%, 5.44%, and 7.28%, which were significantly higher than those of SA-cells and G+SA-cells ($p < 0.05$). While in G+SA-cells, the percentages of palmitic acid (C16:0) (18.12%), linoleic acid (C18:2) (11.01%), and linolenic acid (C18:3) (4.05%) in G+SA-cells were obviously higher than in G-cells and SA-cells. Interestingly, C18:1 showed fluctuation in different carbon sources treatment cells and was especially rich in G+SA-cells by

Table 2 Fatty acid profiles in heterotrophic *C. subellipsoidea* cells treated with different carbon sources

Fatty acid profiles (CX:Y[a])	Relative content (%)		
	G-cells	SA-cells	G+SA-cells
Palmitic acid (C16:0)	10.63±1.18[c]	14.01±1.15[b]	18.12±1.27[a]
Palmitoleic acid (C16:1)	4.40±0.11[a]	3.07±0.12[b]	2.42±0.14[c]
Hexadecadienoic acid (C16:2)	5.44±0.12[a]	2.40±0.04[c]	2.68±0.11[b]
Hexadecatrienoic acid (C16:3)	7.28±0.17[a]	3.12±0.16[b]	2.91±0.13[b]
Oleic acid (C18:1)	33.23±1.41[c]	39.22±1.12[b]	48.69±1.32[a]
Linoleic acid (C18:2)	13.13±0.19[c]	16.50±0.23[b]	11.01±0.21[a]
Linolenic acid (C18:3)	9.90±0.14[c]	5.78±0.16[b]	4.05±0.13[a]
Σ SFA	10.63±1.18[c]	14.01±1.15[b]	18.12±1.27[a]
Σ MUFA	37.63±1.22[c]	42.29±1.09[b]	51.11±1.20[a]
Σ PUFA	35.75±0.13[a]	28.87±0.17[b]	20.65±0.09[c]
TFA	84.01±1.32[c]	85.17±1.08[b]	89.88±1.12[a]
Others	15.99[a]	14.83[b]	10.12[c]

[a]The notation in the form of CX:Y, where X is the carbon number of the fatty acid chain and Y is the number of double bonds. TFA, SFA, MUFA, and PUFA indicated the total fatty acids, saturated fatty acid, monounsaturated fatty acids, and polyunsaturated fatty acids, respectively. *C. subellipsoidea* cells treated with sole 20 g/L of glucose (G), sole 12 g/L of sodium acetate (SA), as well as 20 g/L of G and 12 g/L SA (20G+12SA) were noted as G-cells, SA-cells, and G+SA-cells, respectively. Data are shown as the mean±standard deviation (SD) values for three independent biological replicates ($n=3$). Different letters in the same line indicated significant differences of fatty acids percentages amongst three cells groups ($p < 0.05$)

occupying approximate 48.69% of total FAs, representing 1.24- to 1.47-fold higher than those of G-cells and SA-cells. Another case to commend was that C16:0 occupied the high content in G + SA-cells (18.12%) than in G-cells (10.63%) and SA-cells (14.01%). In addition, the content of C18:3 (4.05%) in G + SA-cells was easily complied with established biodiesel quality specifications (< 12%) by ASTM D-6751 and DINV 14,214. Even though the total fatty acids (TFA) in G + SA-cells showed no noticeable increment compared to sole G or SA, *C. subellipsoidea* cells treated with G + SA carbon source was the preferable fatty acid profiles producer.

The lipid droplets in *C. subellipsoidea* cells treated with glucose combining with sodium acetate

As the transmission electron microscopy results observed in Fig. 2a, a spectacular scene that starch granules occupied almost the entire cell volume whereas only some scattered lipid punctuations was visualized in sole glucose-treated *C. subellipsoidea* cells (G-cells). When algal cells subjected to sole sodium acetate (SA) carbon source treatment, the observed starch granules in number and size were obviously smaller than that of G-cells whilst an increase of lipid bodies in greater quantities showing electron-dense punctuations was observed (Fig. 2b). While in 20 g/L of G and 12 g/L of SA treatment cells (G + SA-cells), the volume of starch grains was obviously less than that of G-cells and SA-cells and also the lipid droplets were polymerized into a big group. These showed consistence with the results shown in "Results" Section that lipid content in G + SA-cells was the highest followed by SA-cells and G-cells.

Metabolites associated with lipid accumulation in *C. subellipsoidea* treated with glucose combining with sodium acetate

A total of 46 intracellular metabolites appointed to starch and sucrose metabolism, tricarboxylic acid cycle (TCA) and glyoxylate shunt metabolism, glutathione metabolism, amino acids metabolism, lipid metabolism, fatty acids biosynthesis, glycerophospholipid metabolism, plant hormones metabolism, inositol phosphate metabolism, and carotenoid biosynthesis were identified by GC-TOF–MS and summarized in Table 3. As shown in Table 3, approximately 85% of the identified metabolites were significantly different amongst sole glucose treatment cells (G-cells), sole sodium acetate treatment cells (SA-cells), and glucose combining with sodium acetate treatment cells (G + SA-cells) ($p < 0.05$). The metabolic samples of G-cells, SA-cells, and G + SA-cells could be clearly separated into three groups in accordance with three types on principal components analysis (PCA) score plot, which indicated the differences of metabolites amongst different carbon source feeding cells. And most individual biological replicate samples tended to be clustered together, representing an overall good reproducibility (Fig. 3a). The supervised clustering partial least squares discriminant analysis (PLS-DA) analysis further indicated that the metabolic profiles of G + SA-cells differ significantly to G-cells and SA-cells (Fig. 3b). PCA and PLS-DA analysis models were well constructed with excellent fit and satisfactory predictive ability ($Q^2 = 0.952$ and $R^2 = 0.992$). The metabolites in variable important in projection (VIP) figure were selected as differential metabolites according to VIP value > 1. As illustrated in Fig. 3c, 21 metabolites with VIP > 1 in the VIP plot, including sucrose, phosphatidylcholine, palmitoyl-*sn*-glycero-3-phosphocholine, malate, glutathione, glycerol, oleic acid, palmitoleoyl
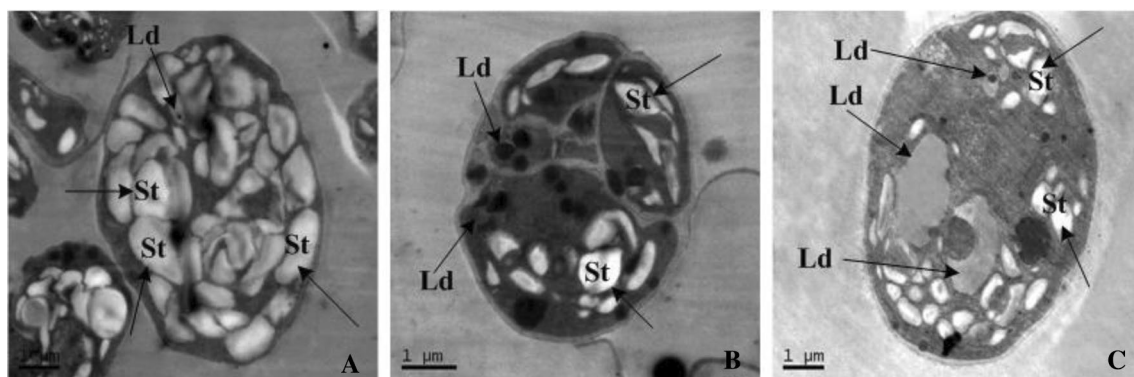

Fig. 2 Transmission electron microscopy of heterotrophic *C. subellipsoidea* cells fed with different carbon sources. **a** Cells treated with sole glucose (20 g/L) carbon source (G-cells); **b** Cells treated with sole sodium acetate (12 g/L) carbon source (SA-cells); **c** Cells treated with the combination of 20 g/L of glucose and 12 g/L of sodium acetate carbon source (G+SA-cells). St and Ld indicated starch granules and lipid droplets, respectively.

Table 3 Global metabolites in heterotrophic *C. subellipsoidea* cells-treated with different carbon sources

Metabolic pathways[a]	Metabolites[b]	Metabolite concentration (mg/g)[c]		
		G-cells	SA-cells	G + SA-cells
Starch and sucrose metabolism	D-Glucose-6-phosphate	1.7694 ± 0.1443^{b}	1.3877 ± 0.4122^{c}	1.8718 ± 0.2122^{a}
	Arabinose	2.5692 ± 0.2122^{a}	1.2612 ± 0.1133^{b}	2.6299 ± 0.1323^{a}
	Xylose	1.5226 ± 0.4022^{b}	0.9306 ± 0.5011^{c}	1.6881 ± 0.3223^{a}
	Sucrose	23.770 ± 3.1140^{b}	8.620 ± 2.4223^{c}	52.56 ± 3.2883^{a}
	Glucoside	1.0095 ± 0.1727^{b}	0.7436 ± 0.1236^{c}	1.1269 ± 0.1775^{a}
	1-Palmitoyl-*sn*-glycero-3-phosphocholine	2.8224 ± 0.5372^{a}	1.9348 ± 0.9950^{b}	2.8468 ± 0.8296^{a}
	1-Stearoyl-*sn*-glycerol-3-phosphocholine	0.6127 ± 0.0040^{a}	0.2392 ± 0.0055^{b}	0.6542 ± 0.1013^{a}
TCA and glyoxylate shunt metabolism	α-Oxoglutarate	1.1197 ± 0.0044^{b}	1.0822 ± 0.0231^{c}	1.2231 ± 0.7722^{a}
	Succinate	1.2722 ± 0.1445^{c}	1.3930 ± 0.5663^{b}	1.5543 ± 0.1445^{a}
	Fumarate	0.1713 ± 0.3200^{b}	0.1764 ± 0.4411^{b}	0.1876 ± 05533^{a}
	Malate	1.6954 ± 0.2322^{c}	2.8224 ± 0.1121^{b}	4.3452 ± 0.7754^{a}
Glutathione metabolism	Glutamate	1.0388 ± 0.5881^{b}	0.8536 ± 0.4772^{c}	3.8897 ± 0.7645^{a}
Amino acids metabolism	Asparagine	1.9876 ± 0.0202^{b}	2.8823 ± 0.1350^{a}	1.5622 ± 0.3334^{c}
	Proline	0.6411 ± 19455^{b}	0.7768 ± 917664^{a}	0.4517 ± 0.1870^{c}
	Aminobutyrate	3.1540 ± 0.3282^{b}	4.2171 ± 0.9921^{a}	2.8699 ± 0.3789^{c}
Lipid metabolism	1,2-Dioleoyl-rac-glycerol	11.5232 ± 1.4332^{c}	13.4674 ± 2.5543^{b}	14.3838 ± 1.2351^{a}
	1-Linoleoyl-rac-glycerol	5.0418 ± 1.0034^{c}	7.4094 ± 1.1234^{b}	9.5294 ± 2.4322^{a}
	1-Linoleoyl glycerol	1.0291 ± 0.1807^{b}	0.7748 ± 0.9014^{c}	1.2204 ± 0.4298^{a}
	Glycerol	9.4846 ± 0.5779^{c}	10.2820 ± 0.4709^{b}	12.0556 ± 0.2580^{a}
	Glucosylceramide	5.5724 ± 0.9922^{c}	6.0168 ± 0.4515^{b}	9.5264 ± 0.1148^{a}
	Adrenoyl ethanolamide	0.8690 ± 0.4145^{b}	1.3540 ± 0.1106^{a}	0.8332 ± 0.2258^{b}
	Palmitoleoyl ethanolamide	20.5810 ± 0.6006^{c}	21.3919 ± 0.1196^{b}	25.1874 ± 0.7272^{a}
	Linolenoyl ethanolamide	2.1092 ± 0.6572^{c}	2.6167 ± 0.3315^{a}	2.2884 ± 0.7474^{b}
Fatty acids biosynthesis	11-Hydroxy-9-tridecenoic acid	5.0003 ± 0.3744^{c}	9.9523 ± 0.7721^{a}	5.1527 ± 0.9933^{b}
	Linoleic acid	1.9410 ± 0.3432^{c}	1.1698 ± 0.5413^{b}	2.7108 ± 0.2724^{a}
	Palmitic acid	10.2594 ± 0.9433^{c}	13.9872 ± 0.1706^{b}	16.8095 ± 0.5566^{a}
	Eicosatrienoic acid	1.6277 ± 0.1211^{b}	1.2414 ± 0.7865^{c}	1.9600 ± 0.3855^{a}
	Stearoylcarnitine	2.7249 ± 0.135^{b}	4.1758 ± 18752^{a}	2.4941 ± 32008^{c}
	Docosatrienoic acid	1.9410 ± 0.3432^{b}	1.1698 ± 0.5413^{c}	2.7108 ± 0.4464^{a}
	9,12,15-Octadecatrienoic acid	1.4164 ± 0.5357^{c}	2.2664 ± 0.9139^{a}	1.8608 ± 0.2478^{b}
	13-Hydroxy-9-methoxy-octadecenoic acid	2.5697 ± 0.1881^{b}	4.2944 ± 0.2443^{a}	2.4206 ± 0.7745^{c}
	Oleic acid	17.6198 ± 0.2105^{c}	30.0641 ± 0.8827^{b}	37.7102 ± 0.4473^{a}
Glycerophospholipid metabolism	Phosphatidic acid	7.7910 ± 0.9922^{a}	6.4857 ± 0.2566^{b}	5.9601 ± 0.3313^{c}
	Diacylglycerol	4.5223 ± 0.4272^{a}	3.0408 ± 0.6525^{b}	2.2742 ± 0.4667^{c}
	Phosphatidylethanolamine	38.0159 ± 1.7857^{a}	24.2326 ± 1.9825^{b}	12.5103 ± 1.9121^{c}
	Phosphatidylcholine	1.6629 ± 0.3595^{a}	1.4124 ± 0.4781^{b}	1.3857 ± 0.3929^{c}
	Phosphatidylserine	1.6362 ± 0.5436^{a}	1.2946 ± 0.8969^{b}	1.4376 ± 0.0464^{c}
	Phosphatidylinositol	74.5792 ± 1.2327^{a}	49.6554 ± 1.8603^{b}	35.7640 ± 1.0867^{c}
	Phosphatidylglycerol	6.4495 ± 0.7471^{a}	3.6009 ± 0.43494^{b}	3.5737 ± 0.9411^{b}
Plant hormones metabolism	Brassinolide	41.9482 ± 2.0981^{b}	38.5263 ± 1.7115^{c}	52.2949 ± 2.4140^{a}
	Pubesenolide	11.7095 ± 1.3733^{c}	12.8564 ± 1.0631^{b}	17.3401 ± 1.8244^{a}
Inositol phosphate metabolism	11'-Carboxy-alpha-chromanol	1.1192 ± 0.8333^{b}	1.0743 ± 0.9697^{c}	1.4280 ± 0.9133^{a}
Carotenoid biosynthesis	β-Cryptoxanthin	2.2129 ± 0.2799^{a}	1.9950 ± 0.7727^{b}	1.5457 ± 0.9869^{c}
	Zeaxanthin	0.8660 ± 0.5066^{a}	0.7915 ± 0.3329^{b}	0.5809 ± 0.9668^{c}
	Citranaxanthin	1.2184 ± 0.6779^{a}	1.0106 ± 0.9773^{b}	0.9184 ± 0.6622^{c}
	Capsanthin 5,6-epoxide	1.8952 ± 0.3244^{a}	1.4957 ± 0.8876^{b}	1.4671 ± 0.7427^{b}

Metabolic pathways (a) and Metabolites (b) were based on https://www.genome.jp/KEGG/pathway.html (KEGG), the human metabolome database (HMDB), and https://metlin.scripps.edu (METLIN); Metabolites concentrations (mg/g)(c) = C × V × M/m, where C was the metabolite concentration (mmol/L), V was the liquid volume of the extracted metabolites (L), M represented the molar mass of each metabolite (g/mol), and m was the weight of each sample (g). The metabolites concentration data are shown as the mean ± SD values for three independent biological replicates. Different letters in the same line indicated significant differences of metabolites concentrations amongst three cells groups ($p < 0.05$)
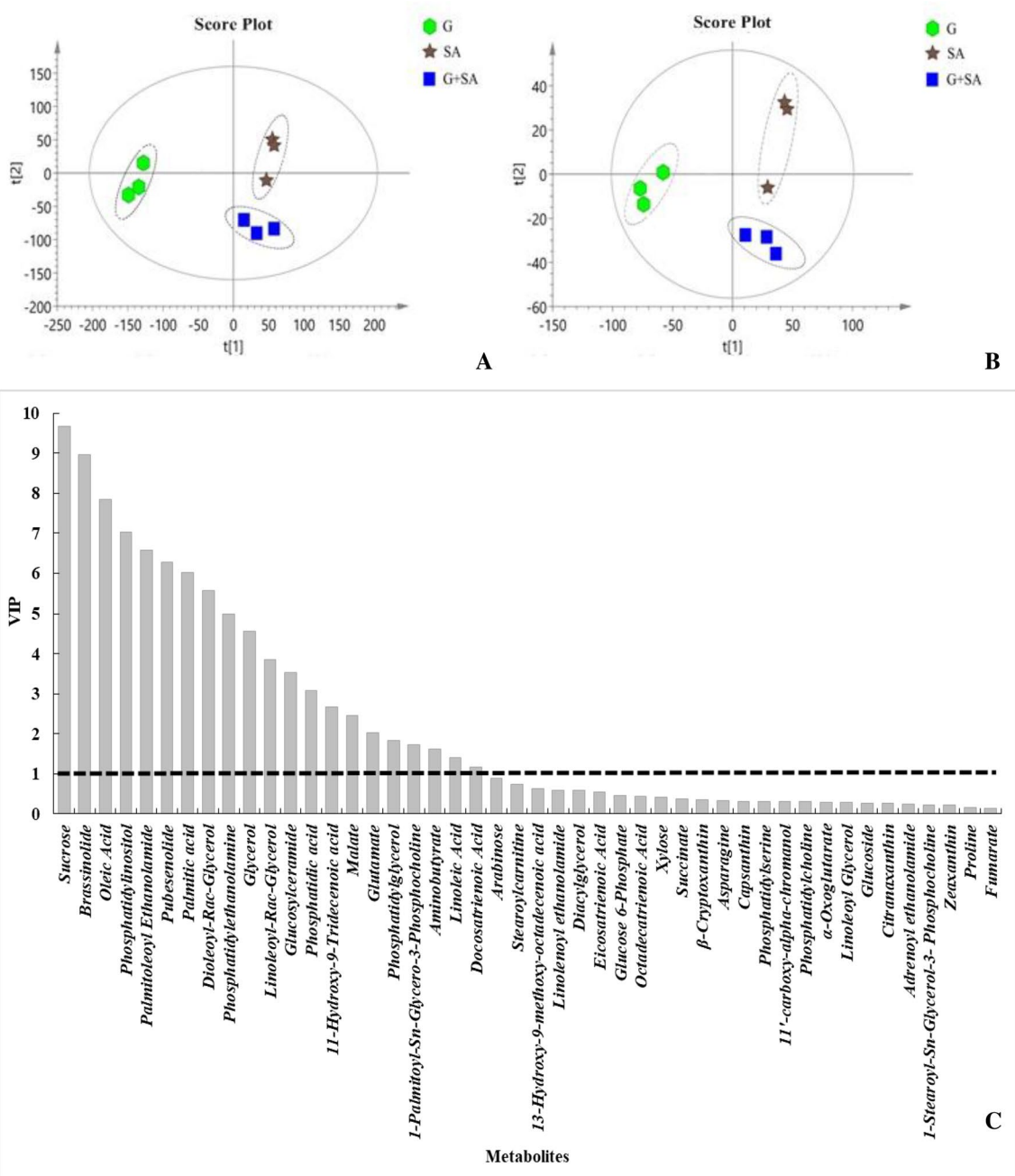
Fig. 3 **a** PCA score plot and **b** PLS-DA score plot of metabolites in heterotrophic *C. subellipsoidea* cells treated with different carbon sources. G-cells, SA-cells, and G + SA-cells were consistent with the footnote shown in Fig. 2. Each symbol represented one biological sample in PCA score plot and PLS-DA score plot as well as the same color and shape dots were biological replicates of individual biological sample. **c** The VIP score plot of metabolites associated with lipid accumulation in *C. subellipsoidea* cells. Metabolites were listed from highest to lowest contributions to lipid accumulation and selected as significant signals according to variables with VIP > 1

ethanolamide, phosphatidyl ethanolamine, brassinolide, pubesenolide, glucose 6-phosphate, and *α*-oxoglutarate were finally determined as important metabolites, which were closely associated with the pathways of lipid and fatty acids biosynthesis or might have crucial effects on lipid accumulation in *C. subellipsoidea* cells.

Discussion

All the benefits (e.g. far higher growth rates and respiration) notwithstanding, glucose (G) substrate still had inherent disadvantages including high energy expenses and costs, contamination and competition by other microorganisms,

inhibition of growth by excess organic substrate (Ren et al. 2016). At this point, the low-cost sodium acetate (SA) could offset some deficiencies of G since it could maintain axenic heterotrophic cultures (Silva et al. 2016). However, the high energy content per mol G was advantages than SA in enhancing the growth rate, the biomass, and ATP generated (Perez-Garcia et al. 2011). Additionally, the biochemical properties of algal strain treated with various carbon source indicated that G functioned as growth promoter and SA as lipid inducer (Cheng et al. 2012). Therefore, developing the combination of G and SA might be mutually-beneficial in enhancing microalgae lipid productivity (Huang et al. 2017). The results of this study shown in Fig. 1 validated the potentials of G combining with SA than sole G or SA in enhancing lipid productivity of *C. subellipsoidea*. The achieved biomass (5.22 g/L) and lipid content (52.16%) by optimal combination of G (20 g/L) and SA (12 g/L) (G + SA) performed better than that of sole G (3.15 g/L and 18.91%) or SA (1.35 g/L and 20.11%) (Fig. 1). The resulting lipid yield (2722.72 mg/L) and lipid productivity (388.96 mg/L/day) by *C. subellipsoidea* cells treated with G + SA was consequently higher than those of sole G (600.04 mg/L and 85.72 mg/L/day) and SA (358.40 mg/L and 51.20 mg/L/day). This obtained lipid yield and lipid productivity were also significantly higher than the reports of Peng et al. (2016) and Yu et al. (2018) where the same *C. subellipsoidea* species was supplemented with 10 g/L crude glycerol or 2% CO_2 to achieve only 1292.04 mg/L

lipid yield and 107.67 mg/L/day lipid productivity as well as 1292.04 mg/L lipid yield and 259.20 mg/L/day lipid productivity, respectively (Table 4). Certainly, the lipid productivity of G + SA in this study performed better than the reports of Breuer et al. (2012) where *C. vulgaris* and *C. zofingiensis* were supplemented with 5% CO_2 to achieve 170 mg/L/day and 301 mg/L/day of lipid productivity. Such fascinating lipid productivity was also competitive with the lipid yield (690.03 mg/L) and lipid productivity (230.01 mg/L/day) by glucose (12 g/L) combining with glycerol (4.1 g/L) for other alga strain *C. vulgaris* (Heredia-Arroyo et al. 2011). Even a mixture of glucose (7.959 g/L), sodium acetate (1.46 g/L), and peptone (7.6 g/L) as well as a combination of glucose (5.78 g/L), peptone (9 g/L), and yeast extract (4.48 g/L) were used for *N. salina* and *T. suecica* species (Azma et al. 2011; Marudhupandi et al. 2016), the achieved lipid productivities were still not as much as *C. subellipsoidea* treated with G + SA carbon source in this study. The above results of this study suggest the ideal combination of *C. subellipsoidea* and G + SA carbon source to ensure the favorable lipid productivity. Moreover, it was worth mentioning that even though the cost of G + SA combining carbon source was higher than that of sole G or SA carbon source, the achieved favorable lipid productivity could easily offset this cost gap, which was extremely advantageous for the economic-feasibility of alga-based biodiesel production.

Not only that the biomass and lipid productivity but also the fatty acids profiles were critical in selecting species

Table 4 Biomass and lipid production of heterotrophic *C. subellipsoidea* in comparison with previous reports of *C. subellipsoidea* and other algal strains

Algal strain	Carbon source	Culture mode	Biomass (g/L)	Lipid yield (mg/L)	Lipid productivity (mg/L/day)	References
C. subellipsoidea	Glucose (20 g/L)	H	4.15	600.04	85.72	This study
C. subellipsoidea	Sodium acetate (12 g/L)	H	1.35	358.40	51.20	This study
C. subellipsoidea	Glucose (20 g/L) and sodium acetate (12 g/L)	H	5.22	2722.72	388.96	This study
C. subellipsoidea	Crude glycerol (10 g/L)	H	7.62	2073.6	259.20	Yu et al. (2018)
C. subellipsoidea	2% CO_2	P	2.66	1292.04	107.67	Peng et al. (2016)
C. vulgaris	Glucose (12 g/L) and glycerol (4.1 g/L)	M	5.62	690.03	230.01	Heredia-Arroyo et al. (2011)
N. salina	Glucose (7.96 g/L), sodium acetate (1.46 g/L), and peptone (7.6 g/L)	P	8.40	–	–	Azma et al. (2011)
T. suecica	Glucose (5.78 g/L), peptone (9 g/L), and yeast extract (4.48 g/L)	H	1.85	631.8	48.6	Marudhupandi et al. (2016)
C. vulgaris	5% CO_2	P	3.43	1700	170	Breuer et al. (2012)
C. zofingiensis	5% CO_2	P	4.69	2408	301	Breuer et al. (2012)

P photoautotrophic, *H* heterotrophic, *M* mixotrophic

– Indicated this value was not shown in this reference

for scale-up alga-based biodiesel production (Nascimento et al. 2013). Interestingly, the fatty acid profiles of lipids in G + SA-cells had several ravishing performances, including (1) the lipids were endowed with C16-C18 long-chain fatty acid groups, accounting for 89.88% of the total fatty acids (2) the high proportion of monounsaturated oleic acid (C18:1) occupied nearly 50% of total fatty acids, which was higher than the reported 15.57% in *C. subellipsoidea* cells treated with CO_2 (Peng et al. 2016) and even much higher than that of 3.88% in *C. subellipsoidea* cells treated with crude glycerol (Yu et al. 2018) (3) a certain proportion (> 20.65%) of polyunsaturated fatty acids (PUFAs) containing greater than two double bonds. These characteristics of fatty acids profiles meet with the promising feedstock for high-quality biodiesel production. G + SA combination treatment also positively regulated the proportions of saturated fatty acid (SFA) (e.g. C16:0) to render the content of SFA (18.12%) and MUFAs (51.11%) over PUFAs (20.65%). Such high proportions of SFAs and MUFAs in lipids were usually beneficial in enhancing energy yield and endowing superior oxidative stability of alga-based biodiesel production. However, lipids dominated by SFAs and MUFAs tended to cause solidify whilst lipids rich in PUFAs usually had very good performance on the cold flow property but more susceptible to oxidation (Ebrahimian et al. 2014). The proportions of MUFAs exceeding the summation of SFAs and PUFAs could balance superior oxidation stability and lower viscosity of alga-based biofuels (Knothe 2014). Only the percentage of MUFAs in G + SA-cells was higher than the summation of SFAs and PUFAs, which indicated that the fatty acids profiles of G + SA-cells would provide excellent fuel characteristics for alga-based biodiesel. Additionally, linolenic acid (C18:3) should also be taken into consideration to secure the quality of alga-based biodiesel. It could be seen from Table 2 that the percentage of C18:3 (4.05%) in G + SA-cells easily complied with the specification (< 12%) established by ASTM D-6751 and EN 14,214. These again indicated the potential of *C. subellipsoidea* treated with G + SA combining carbon source in producing preferable fatty acids to guarantee algae-based biodiesel production.

The potential possibilities of lipid accumulation triggered by G + SA carbon source was the premise to further improve the lipid productivity of *C. subellipsoidea* and provide consulting for the application of this combining strategy in other algae species. As listed in Table 3, some metabolites linking starch, sucrose, and glucose metabolism processes including 1-palmitoyl-*sn*-glycero-3-phosphocholine, D-glucose-6-phosphate, 1-stearoyl-*sn*-glycerol-3-phosphocholine, arabinose, xylose, sucrose, and glucoside were found in *C. subellipsoidea* cells. The levels of most of these metabolites in G-cells especially in G + SA-cells were generally higher than in SA-cells, reflecting that glycolysis pool was significantly activated in G-cells and more intermediates (e.g.

pyruvate and acetyl-CoA) were used to support the cells growth or lipid biosynthesis. However, it could be seen from Fig. 1 that the lipid content in G-cells was not higher than in SA-cells even much less than G + SA-cells while the biomass of G-cells was really higher than that of SA-cells. This indicated that a large proportion of acetyl-CoA from glycolysis in G-cells might flow into TCA cycle while not into fatty acids pathway to generate energy for cell proliferation.

It was well-documented that acetate was usually oxidized metabolically through glyoxylate cycle to form malate and further acetyl-CoA resulting in the deposition of carbon as lipids or TCA cycle to mainly provide energy as ATP for metabolic growth (Perez-Garcia et al. 2011; Puzanskiy et al. 2018). Interestingly, several common intermediates (e.g. succinate, fumarate, and malate) of both cycles (glyoxylate cycle and TCA cycle) were up-regulated while α-oxoglutarate involved in exclusive TCA cycle showed reduction in SA-cells compared to G-cells. In addition, some amino acid metabolites (asparagine, proline, and aminobutyrate) that could be synthesized by intermediates in TCA cycle showed significant accumulation in SA-cells. This indicated that the intermediates in TCA might be largely converted into amino acids and TCA cycle was down-regulated response to SA treatment. Relying on the variations of metabolites involved in glyoxylate cycle and TCA cycle, it could be speculated that acetate was mainly metabolized through glyoxylate cycle to form more acetyl-CoA for lipid biosynthesis in SA-cells. This exactly catered to the results of this study that *C. subellipsoidea* cells supplemented with SA showed the lower biomass (1.35 g/L) and the high lipid content (24.55%) (Fig. 1). Collectively, G promoted glycolysis and drove acetyl-CoA into TCA cycle for metabolic growth while SA activated intracellular glyoxylate shunt to contribute acetyl-CoA for lipid accumulation in *C. subellipsoidea* cells. This agreed with the conclusion of Cheng et al. (2012) where G was regarded as growth promoter and SA was regarded as lipid inducer.

As shown in Fig. 1, although G and SA used in G + SA combining carbon sources were consistent concentrations with the sole G or SA, the achieved biomass and lipid content in *C. subellipsoidea* cells fed with G + SA were higher than that of G-cells and SA-cells. This might be due to that G + SA combining treatment reallocated energy or intermediates and also further optimized some metabolic pathways associated with growth and lipid biosynthesis to eventually improve the lipid productivity. These favorable metabolic variations in promoting lipid productivity of G + SA-cells were mainly reflected in (1) The levels of most metabolites associated with glycolysis particularly sucrose in G + SA-cells were significantly higher than that of G-cells and SA-cells ($p < 0.05$) (Table 3), which indicated that glycolysis was more active in G + SA-cells. This would cause the more accumulation of intermediates (e.g. pyruvate, malate, and

succinate) of energetic pathways consequently increased the biomass and lipid content of G + SA-cells. (2) G + SA combining treatment induced *C. subellipsoidea* cells to synthesize the high content of glutamate, which could be directly converted into α-oxoglutarate to increase TCA cycle. Not only this metabolite exclusively belonging to TCA cycle showed up-regulation but also the levels of succinate, fumarate, and malate assigned to both of glyoxylate cycle and TCA cycle were higher than in G-cells and SA-cells. These indicated that both of glyoxylate cycle and TCA cycle might be concurrently elevated in G + SA-cells consequently the resulting high biomass and lipid content. (3) G + SA combining treatment up-regulated some intermediates closely related to lipid pathway particularly 1,2-dioleoyl-rac-glycerol, 1-linoleoyl-rac-glycerol, glycerol, glucosylceramide, and palmitoleoyl ethanolamide to enable the lipid level in G + SA-cells higher than that G-cells and SA-cells. Yang et al. (2018) reported that SA addition increased the contents of tridecenoic acid, palmitic acid, and oleic acid consequently resulted in the high lipid yield of *C. reinhardtii*. Therefore, it could be concluded that the up-regulations of these fatty acids in G + SA-cells significantly contributed to lipid accumulation in *C. subellipsoidea* cells. (4) The carbon skeleton feedstock including phosphatidyl-choline (PC), phosphatidyl-inositol (PI), phosphatidyl-ethanolamine (PE), phosphatidic acid (PA), diacylglycerol (DG), phosphatidyl-serine (PS), and phosphatidyl-glycerol (PG) used for membrane lipids biosynthesis showed down-regulation in G + SA-cells, especially PE and PI were 2.08- to 3.04-fold less than that of G-cells and SA-cells. The previous report of Trentacoste et al. (2013) have provided evidence that membrane lipids could achieve mutual transformations with *de novo* TAG synthesis in higher plants. Therefore, the reduction of these metabolites indicated the membrane lipids pool were converted into TAG accumulation in G + SA-cells and this was consistent with the results of Fig. 2 where lipid droplets were polymerized into a big group in G + SA-cells while only scattered lipid punctuations was visualized in G-cells and SA-cells.

Metabolites were grouped in several blocks in the light of direct or indirect contributions to growth and lipid accumulation in *C. subellipsoidea* cells. The above elaborated the predominance of direct metabolites associated with the biomass and lipid content. Actually, the indirect metabolite pools also played key roles in systemic metabolic rearrangements of growth and lipids accumulation. It has been reported that brassinolide exhibited extensive physiological effects on plant development (e.g. growth) and presented new opportunities in developing alga-based biodiesel production (Lu and Xu 2015; Liu et al. 2016). Therefore, it could be concluded that the elevated level of brassionlide (53.29 mg/g) by G + SA combining treatment might be critical in regulating simultaneous cell growth and lipid biosynthesis in

C. subellipsoidea. The concentration of another important metabolite (i.e. 11′-carboxy-alpha-chromanol) involved in inositol phosphate metabolism showed also increment in G + SA-cells than in G-cells and SA-cells. Previous work has shown an up-regulation of chromanol in response to oxidative stress to sustain plant cell growth (Kruk et al. 2016). Therefore, the enhanced chromanol in G + SA-cells in this study might play an important role in an effort to support cell growth. Additionally, some intermediates located in carotenoid biosynthesis pathway including β-cryptoxanthin, zeaxanthin, citranaxanthin, and capsanthin 5,6-epoxide were also identified in *C. subellipsoidea* cells (Table 3). While the accumulation levels of most of these metabolites in G + SA-cells were less than that of G-cells and SA-cells. Araya et al. (2014) once proposed the competition relationship between carotenoid and lipids biosynthesis in three *Chlorella* species. Thus, the down-regulations of these metabolites involved in carotenoid biosynthesis implied that more carbon metabolic flux and precursors were drove into lipid-related pathways to support lipid accumulation in G + SA-cells. Finally, although the identified pubesenolide was assigned to plant hormones metabolism and showed significant up-regulation in G + SA-cells, the precise functions of this metabolite were mostly unknown. It was believed that the regulatory functions of pubesenolide would be revealed with the development of indispensable molecular tools for microalgal gene characterization.

Conclusion

The potential superiority of the combination of glucose and sodium acetate (G + SA) versus sole glucose (G) or sole sodium acetate (SA) feeding was to give a win–win for both biomass and lipid biological indicators of *C. subellipsoidea*. The fatty acid profiles (mainly C16–C18 long-chain groups) and the proportion of preferable fatty acid (e.g. C18:1) in G + SA-cells rendered algae-based biofuels to easily comply with the established quality specifications of biodiesel. G + SA combining treatment promoted glycolysis as well as activated glyoxylate shunt and TCA cycle to support such fascinating lipid accumulation. Consistent efforts or improvements including further exploring low-cost SA from waste anaerobic digestion process and the combinations of other carbon sources even nitrogen sources were still be devoted before impelling such conducive strategy for other microalgae strains and toward offsetting alga-based biodiesel cost.

References

Allen JW, Dirusso CC, Black PN (2015) Triacylglycerol synthesis during nitrogen stress involves the prokaryotic lipid synthesis pathway and acyl chain remodeling in the microalgae *Coccomyxasubellipsoidea*. Algal Res 10:110–120

Allen JW, Dirusso CC, Black PN (2017) Carbon and acyl chain flux during stress-induced triglyceride accumulation by stable isotopic labeling of the polar microalga *Coccomyxasubellipsoidea* C169. J Biol Chem 292:361–374

Araya B, Gouveia L, Nobre B, Reis A, Chamy R, Poirrier P (2014) Evaluation of the simultaneous production of lutein and lipids using a vertical alveolar panel bioreactor for three *Chlorella* species. Algal Res 6:218–222

Azma M, Mohamed MS, Mohamad R, Abdul Rahim R, Ariff AB (2011) Improvement of medium composition for heterotrophic cultivation of green microalgae, *Tetraselmis suecica*, using response surface methodology. Biochem Eng J 53:187–195

Breuer G, Lamers PP, Martens DE, Draaisma RB, Wijffels RH (2012) The impact of nitrogen starvation on the dynamics of triacylglycerol accumulation in nine microalgae strains. Bioresour Technol 185:217–226

Cheng JS, Niu YH, Lu SH, Yuan YJ (2012) Metabolome analysis reveals ethanolamine as potential marker for improving lipid accumulation of model photosynthetic organisms. J Chem Technol Biot 87:1409–1418

Demirbas A (2010) Use of algae as biofuel sources. Energy Convers Manag 51:2738–2749

Ebrahimian A, Kariminia HR, Vosoughi M (2014) Lipid production in mixotrophic cultivation of *Chlorella vulgaris* in a mixture of primary and secondary municipal wastewater. Renew Energy 71:502–508

Heredia-Arroyo T, Wei W, Ruan R, Hu B (2011) Mixotrophic cultivation of *Chlorella vulgaris* and its potential application for the oil accumulation from non-sugar materials. Biomass Bioenergy 35:2245–2253

Huang AY, Sun LL, Wu SC, Liu CX, Zhao PP, Xie XJ, Wang GC (2017) Utilization of glucose and acetate by *Chlorella* and the effect of multiple factors on cell composition. J Appl Phycol 29:23–33

Knothe G (2014) A comprehensive evaluation of the cetane numbers of fatty acid methyl esters. Fuel 119:6–13

Kruk J, Szymańska R, Nowicka B, Dłużewska J (2016) Function of isoprenoid quinones and chromanols during oxidative stress in plants. New Biotechnol 33:636–643

Liu ZL, Li L, Luo ZS, Zeng FF, Jiang L, Tang KC (2016) Effect of brassinolide on energy status and proline metabolism in postharvest bamboo shoot during chilling stress. Postharvest Biol Technol 111:240–246

Lu YD, Xu J (2015) Phytohormones in microalgae: a new opportunity for microalgal biotechnology? Trends Plant Sci 20:273–282

Marudhupandi T, Sathishkumar R, Kumar TTA (2016) Heterotrophic cultivation of *Nannochloropsis salina* for enhancing biomass and lipid production. Biotechnol Rep 10:8–16

Mu JX, Li ST, Chen D, Xu H, Han FX, Feng B, Li YQ (2015) Enhanced biomass and oil production from sugarcane bagasse hydrolysate (SBH) by heterotrophic oleaginous microalga *Chlorella protothecoides*. Bioresour Technol 185:99–105

Nascimento IA, Marques SSI, Cabanelas ITD, Pereira SA, Druzian JI, Souza CO, Vich DV, de Carvalho GC, Nascimento MA (2013) Screening microalgae strains for biodiesel production: lipid productivity and estimation of fuel quality based on fatty acids profiles as selective criteria. Bioenergy Res 6:1–13

Oh YK, Hwang KR, Kim C, Kim JR, Lee JS (2018) Recent developments and key barriers to advanced biofuels: A short review. Bioresour Technol 257:320–333

Palabhanvi B, Muthuraj M, Mukherjee M, Kumar V, Das D (2016) Process engineering strategy for high cell density-lipid rich cultivation of *Chlorella* sp. FC2 IITG via model guided feeding recipe and substrate driven pH control. Algal Res 16:317–329

Peng HF, Dong W, Gu C, Chen F (2016) Transcriptome analysis reveals global regulation in response to CO_2 supplementation in oleaginous microalga *Coccomyxa subellipsoidea* C-169. Biotechnol Biofuels 9:151

Perez-Garcia O, Escalante FM, de-Bashan LE, Bashan Y (2011) Heterotrophic cultures of microalgae: metabolism and potential products. Water Res 45:11–36

Puzanskiy R, Tarakhovskaya E, Shavarda A, Shishova M (2018) Metabolomic and physiological changes of *Chlamydomonas reinhardtii* (Chlorophyceae, Chlorophyta) during batch culture development. J Appl Phycol 30:803–818

Ren XJ, Chen JK, Deschênes JS, Tremblay R, Jolicoeur M (2016) Glucose feeding recalibrates carbon flux distribution and favours lipid accumulation in *Chlorella protothecoides* through cell energetic management. Algal Res 14:83–91

Shuba ES, Kifle D (2018) Microalgae to biofuels: 'Promising' alternative and renewable energy, review. Renew Sustain Energy Rev 81:743–755

Silva HR, Prete CEC, Zambrano F, de Mello VH, Tischer CA, Andrade DS (2016) Combining glucose and sodium acetate improves the growth of *Neochloris oleoabundans* under mixotrophic conditions. AMB Expr 6:10

Trentacoste EM, Shrestha RP, Smith SR, Glé C, Hartmann AC, Hildebrand M, Gerwicka WH (2013) Metabolic engineering of lipid catabolism increases microalgal lipid accumulation without compromising growth. Proc Natl Acad Sci USA 110:19748–19753

Wang SK, Wang X, Tao HH, Sun XS, Tian YT (2018) Heterotrophic culture of *Chlorellapyrenoidosa* using sucrose as the sole carbon source by co-culture with immobilized yeast. Bioresour Technol 249:425–430

Wen QX, Chen ZQ, Li PF, Duan R, Ren NQ (2013) Lipid production for biofuels from hydrolyzate of waste activated sludge by heterotrophic *Chlorella protothecoides*. Bioresour Technol 143:695–698

Yang L, Chen J, Qin S, Zeng M, Jiang YG, Hu L, Xiao P, Hao WL, Hu ZL, Lei AP, Wang JX (2018) Growth and lipid accumulation by different nutrients in the microalga *Chlamydomonasreinhardtii*. Biotechnol Biofuels 11:40

Yu ZY, Liu L, Chen JH, Wang XP, Wei D (2018) Effect of crude glycerol on heterotrophic growth of *Chlorella pyrenoidosa* and *Coccomyxa subellipsoidea* C-169. J Appl Phycol 30:2989–2996